

1 Supplementary Information

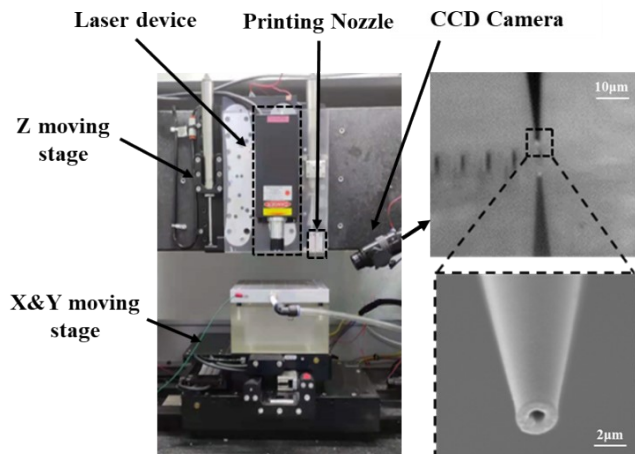
2

3 **Laser-assisted electrohydrodynamic printing of sub-microscale 3D conductive** 4 **features on low-melting-point polymeric substrates**

5 *Jiaxin Li^{1,2,3}, Jinke Chang⁴, Yuhua Chen^{1,2,3}, Qihang Ma^{1,2,3}, Kun Yu^{1,2,3}, Yi Ding^{1,2,3}, Dichen*

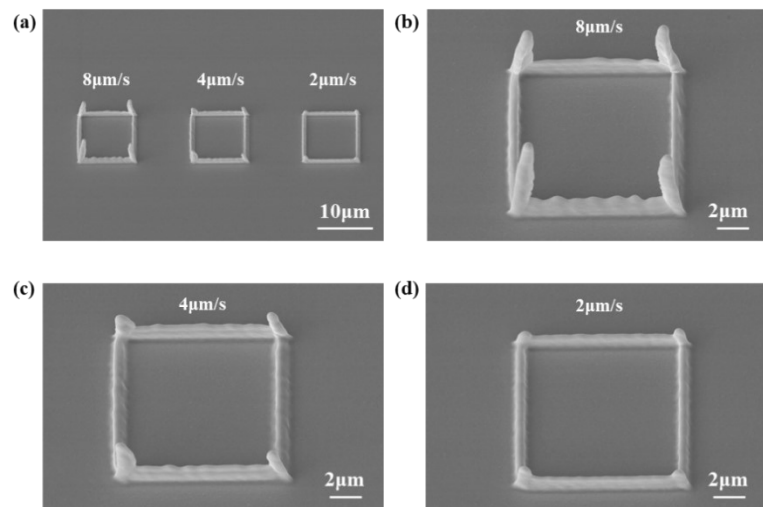
6 *Li^{1,2,3}, Jiankang He^{1,2,3 *}*

7



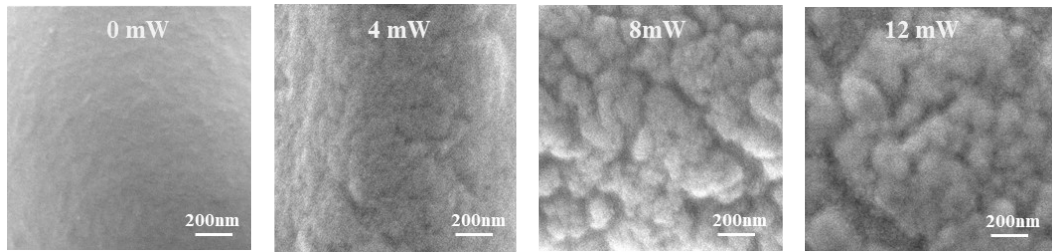
8

9 **Figure S1.** Laser-assisted EHD printing system.

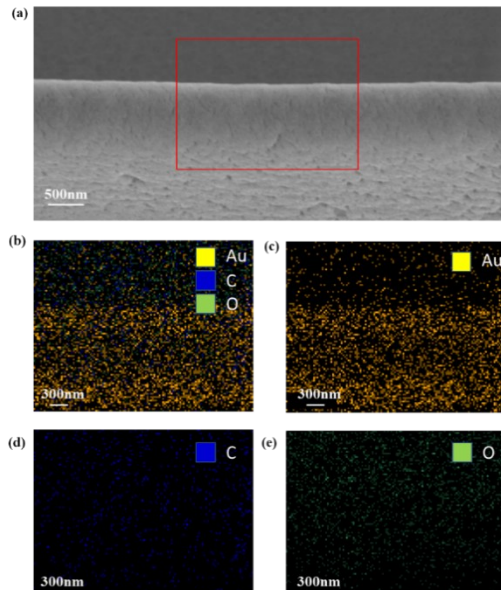


10

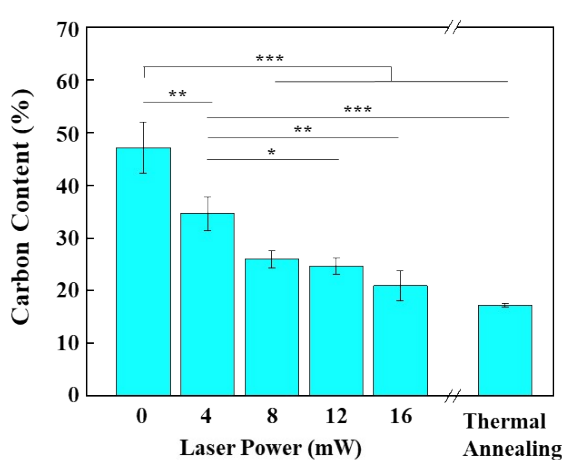
11 **Figure S2.** EHD printed a sub-microscale wall with different printing speeds.



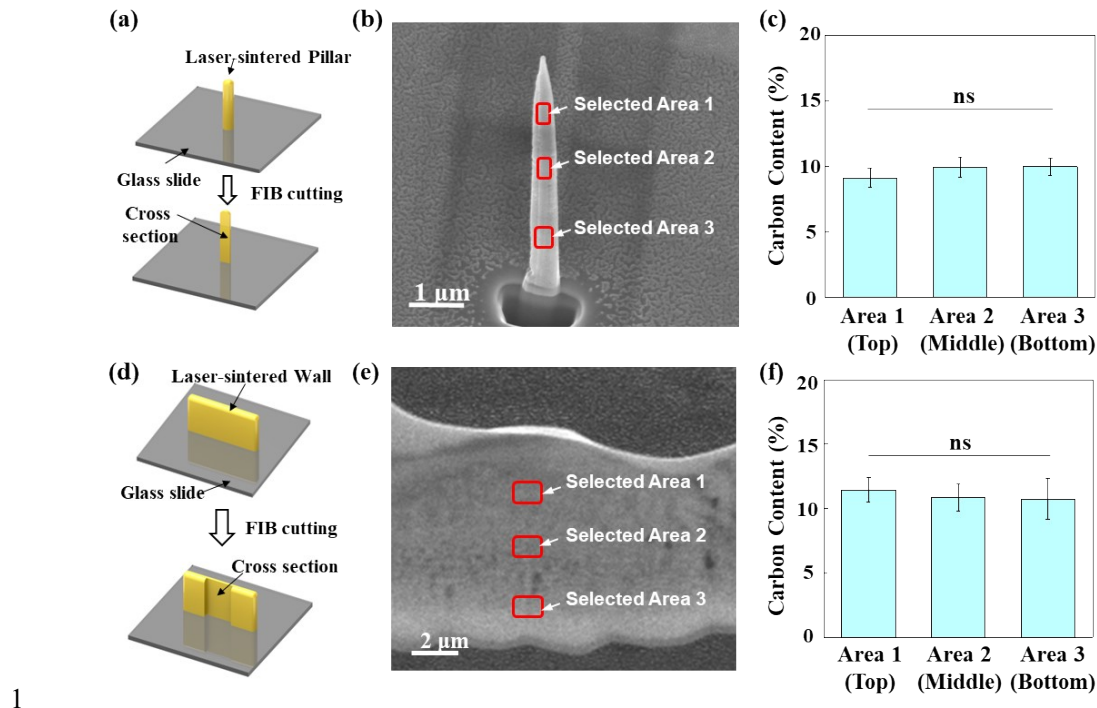
1 **Figure S3.** SEM image of surface morphology of EHD-printed wall sintered with laser powers
2 of 0, 4, 8, and 12 mW.



4 **Figure S4.** Energy dispersive X-ray spectroscopy (EDX) maps of the printed wall.



6 **Figure S5.** Effect of laser power on the carbon content of EHD-printed structures measured by X-ray Photoelectron Spectroscopy (XPS) (mean \pm s.d., $n = 3$). Statistical comparisons were conducted using one-way Analysis of Variance with Tukey's test to determine statistical significance among multiple groups. The levels of significance were established at * $P < 0.05$, ** $P < 0.01$, *** $P < 0.001$.

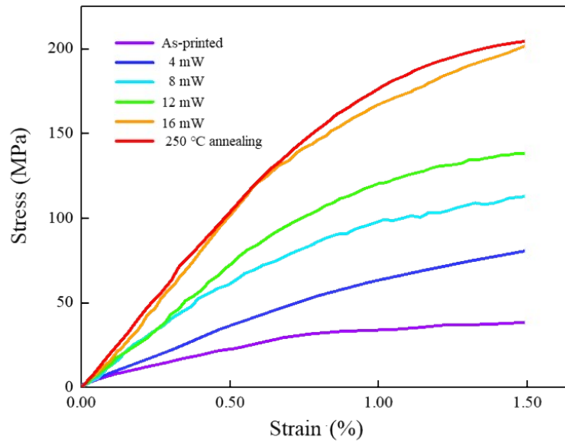


1

2 **Figure S6.** Carbon content across the cross-section of different printed structures. (a) Schematic of
3 the laser-sintered pillar sectioned longitudinally by via Focused Ion Beam (FIB). (b) SEM image of
4 the cross-section of the laser-sintered pillar and the selected area at different heights. (c) Carbon
5 content of the chosen areas (mean \pm s.d., n = 3). (d) Schematic of the laser-sintered wall sectioned
6 longitudinally by FIB. (e) SEM image of the cross-section of the laser-sintered wall and the selected
7 area at different heights. (f) Carbon content of the chosen areas (mean \pm s.d., n = 3). Statistical
8 comparisons were performed using one-way Analysis of Variance with Tukey's tests to assess
9 significance among multiple groups, and no significant differences were observed (ns).

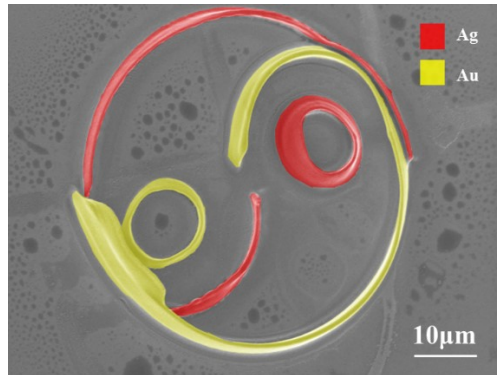
10

11 **Figure S7.** Infrared thermal images depict the laser spot during the laser sintering of gold
12 nanoparticle ink at varied laser powers. To facilitate infrared observation, the laser spot was
13 intentionally defocused and enlarged to approximately 40 μm. Accordingly, the laser power was
14 increased by a factor of 16 from the labeled value to maintain a constant power density.



1

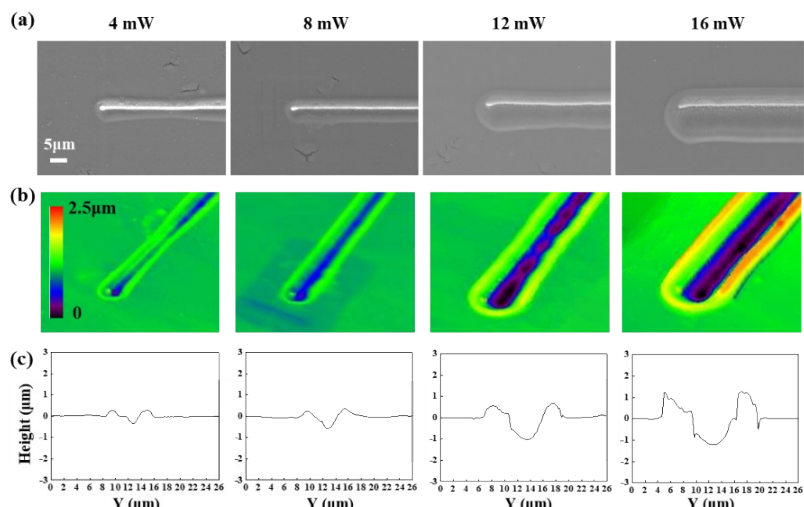
2 **Figure S8.** Stress–strain curves of the printed micropillars, showing the mechanical performance
 3 achieved by *in-situ* laser sintering (across a range of powers) versus conventional thermal sintering
 4 at 250 °C.



5

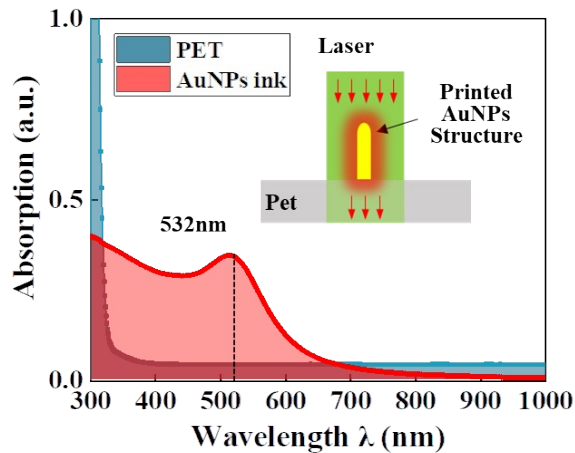
6 **Figure S9.** Multimaterial Taiji pattern printed by laser-assisted EHD printing.

7



8

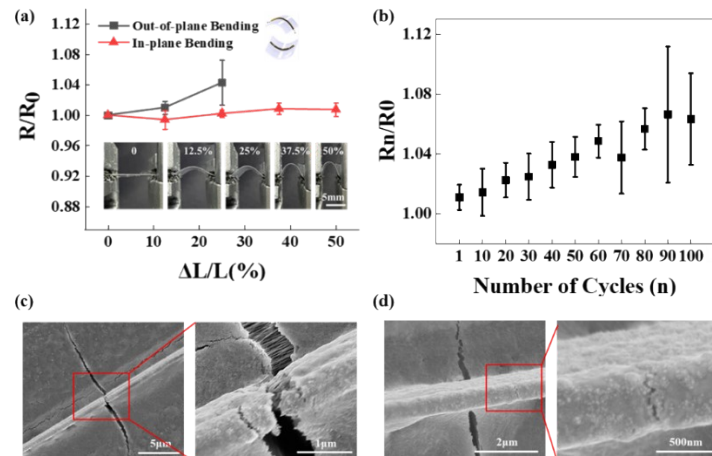
9 **Figure S10.** Effect of laser sintering on PET film. (a) SEM images of the laser-sintered sub-
 10 microscale electrode on PET film with laser powers of 4, 8, 12, and 16 mW. (b) Microscopic images
 11 of the laser-sintered sub-microscale electrode on PET film with various laser powers. (c) Cross-
 12 section of laser-sintered sub-microscale electrode on PET film with various laser powers.



1

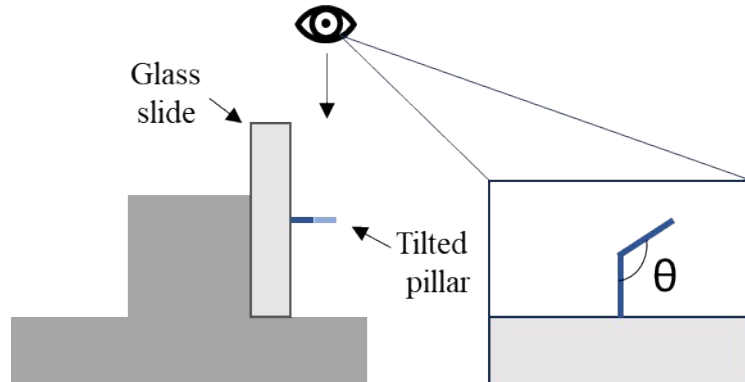
2 **Figure S11.** Absorption spectroscopy of PET film and AuNPs ink.

3



4

5 **Figure S12.** Cyclic mechanical testing of printed gold lines on PET film.



6

7 **Figure S13.** Schematic of SEM observation and tilting angle measurement for printed pillars.

8

Printed Structure	Nozzle diameter	Gas pressure	Peak Voltage	Voltage Frequency	Duty Ratio	Nozzle-to-collector distance	Printing Speed
Micropillar	1 μm	34 mbar	250	1 kHz	50%	15 μm	X/Y axis: 0 nm/s Z axis: 0 or 400 nm/s
Tilted micropillar	1 μm	34 mbar	250	1 kHz	50%	15 μm	X/Y axis: 100-600 nm/s Z axis: 0 nm/s
Microwall	1 μm	34 mbar	250	1 kHz	50%	15 μm	X/Y axis: 800 nm/s Z axis: 0 nm/s

2 **Table S1.** Summary of the EHD printing parameters for different printed structures in this study.

Figure Number	Laser spot diameter	Laser power	Laser scanning speed
Figure 3a,e	10 μm	0, 4, 8, 12, 16 mW	1 mm/s
Figure 3c	10 μm	8 mW	1 mm/s
Figure 4b	10 μm	4, 8, 12, 16 mW	0.1, 1, 10 mm/s
Figure 4c	10 μm	0, 4, 8, 12 mW	1 mm/s
Figure 4d,e	10 μm	0, 4, 8, 12, 16 mW	1 mm/s
Figure 4g	40 μm	64, 128, 192, 256 mW	1 mm/s
Figure 5b	10 μm	0, 4, 8, 12, 16 mW	1 mm/s
Figure 5d	10 μm	8 mW	1 mm/s
Figure 6	10 μm	8 mW	1 mm/s

4 **Table S2.** Summary of the laser sintering parameters employed for the printed structures throughout
5 the figures.